Physics Letters B 687 (2010) 320–326

Contents lists available at ScienceDirect

Physics Letters B

www.elsevier.com/locate/physletb

ϕ-meson production in In–In collisions at $E_{\rm lab} = 158A$ GeV: Evidence for relics of a thermal phase

E. Santini [a,*], H. Petersen [b], M. Bleicher [c]

[a] Institut für Theoretische Physik, Goethe-Universität, Max-von-Laue-Str. 1, D-60438 Frankfurt am Main, Germany
[b] Department of Physics, Duke University, Durham, NC 27708-0305, United States
[c] Frankfurt Institute for Advanced Studies (FIAS), Ruth-Moufang-Str. 1, D-60438 Frankfurt am Main, Germany

ARTICLE INFO

Article history:
Received 6 October 2009
Received in revised form 9 February 2010
Accepted 27 February 2010
Available online 17 March 2010
Editor: J.-P. Blaizot

Keywords:
Monte Carlo simulations
Relativistic heavy-ion collisions
Particle and resonance production

ABSTRACT

Yields and transverse mass distributions of the ϕ-mesons reconstructed in the $\phi \to \mu^+\mu^-$ channel in In+In collisions at $E_{\rm lab} = 158A$ GeV are calculated within an integrated Boltzmann+hydrodynamics hybrid approach based on the Ultrarelativistic Quantum Molecular Dynamics (UrQMD) transport model with an intermediate hydrodynamic stage. The analysis is performed for various centralities and a comparison with the corresponding NA60 data in the muon channel is presented. We find that the hybrid model, that embeds an intermediate locally equilibrated phase subsequently mapped into the transport dynamics according to thermal phase-space distributions, gives a good description of the experimental data, both in yield and slope. On the contrary, the pure transport model calculations tend to fail in catching the general properties of the ϕ meson production: not only the yield, but also the slope of the m_T spectra, compare poorly with the experimental observations at top SPS energies.

1. Introduction

The production of ϕ mesons is considered to be one of the key observables to probe the state of matter produced in relativistic heavy-ion collisions. Strangeness enhancement in relativistic nucleus–nucleus collisions compared to nucleon–nucleon collisions has been originally suggested as a possible signal for the formation of a deconfined plasma of quarks and gluons during the initial state of the reaction [1–3]. The dominant production of $s\bar{s}$ pairs via gluon–gluon interaction in the plasma may result in an enhanced number of strange and multistrange particles produced after hadronization; in particular, free $s\bar{s}$ pairs would coalesce to form ϕ mesons [3], whereas their production in pp collisions is suppressed according to the Okubo–Zweig–Iizuka rule [4–6]. It is moreover expected that ϕ mesons decouple from the rest of the system earlier than other non-strange hadrons. At RHIC energies, an early decoupling of the ϕ from the hadronic rescattering dynamics was found in Refs. [7] and [8]. Similar conclusions were obtained with the RQMD cascade in [9] for the Ω baryons at SPS energies.

The dominant hadronic decay of the ϕ meson is $\phi \to K\bar{K}$; additionally, being a neutral vector meson, the ϕ contributes to dilepton production via the direct decays $\phi \to e^+e^-$ and $\phi \to \mu^+\mu^-$. Phi meson production was investigated extensively at the SPS by several experiments in the kaon (NA49 [10–13] and CERES [14]), dielectron (CERES [14]), and dimuon (NA50 [15] and NA60 [16]) channels. The reconstruction of in-matter $\phi \to K\bar{K}$ decays, however, might be partially prevented by kaon absorption and rescattering [17–19] and a priori a careful investigation of kaon final state interactions cannot be avoided in a quantitative comparison to experimental data. On the contrary, the dilepton channel is not affected by such a shortcoming: dileptons leave their production site essentially undistorted, and a comparison of model calculations to measurements in the dilepton channel is surely more straightforward. Recently, high statistics measurements of $\phi \to \mu^+\mu^-$ meson production in In–In collisions at $E_{\rm lab} = 158A$ GeV have been presented by the NA60 Collaboration [16]. This reaction will be addressed in the present work.

To investigate $\phi \to \mu^+\mu^-$ production in In–In collisions at $E_{\rm lab} = 158A$ GeV we employ an integrated Boltzmann+hydrodynamics hybrid approach based on the Ultrarelativistic Quantum Molecular Dynamics (UrQMD) transport model with an intermediate hydrodynamic stage. In this approach, initial conditions and continuous decoupling up to freeze-out are treated within a full non-equilibrium transport approach, whereas hydrodynamics is used to describe the intermediate equilibrated phase. This allows to reduce the parameters for the initial conditions and provides a consistent freeze-out description. Moreover, by comparing the hybrid approach to pure transport calculations, we are able to directly investigate the consequences that a dynamical approach

* Corresponding author.
E-mail address: santini@th.physik.uni-frankfurt.de (E. Santini).

0370-2693/$ – see front matter
doi:10.1016/j.physletb.2010.02.085

involving local thermal and chemical equilibrium and one based on full non-equilibrium dynamics have on ϕ meson production.

The Letter is structured in the following way. In Section 2, we briefly discuss the hybrid model and present the procedure used to evaluate the $\phi \to \mu^+\mu^-$ emission and, consequently, reconstruct the ϕ meson. In Section 3 we present calculations for ϕ-meson transverse mass spectra as a function of centrality. The various contributions to the spectra associated with different stages of the reaction dynamics are shown and a comparison to the NA60 data is presented. Finally, a summary and conclusions are given in Section 4.

2. The model

2.1. The hybrid approach

To simulate the dynamics of the In+In collisions we employ a transport approach with an embedded three-dimensional ideal relativistic one fluid evolution for the hot and dense stage of the reaction based on the UrQMD model [20]. The present hybrid approach has been extensively described in Ref. [20]. Here, we limit ourselves to briefly describe its main features and refer the reader to Ref. [20] for details.

UrQMD [21–23] is a hadronic transport approach which simulates multiple interactions of ingoing and newly produced particles, the excitation and fragmentation of color strings and the formation and decay of hadronic resonances. The coupling between the UrQMD initial state and the hydrodynamical evolution proceeds when the two Lorentz-contracted nuclei have passed through each other. Here, the spectators continue to propagate in the cascade and all other hadrons are mapped to the hydrodynamic grid. This treatment is especially important for non-central collisions which are also studied in the present work. Event-by-event fluctuations are directly taken into account via initial conditions generated by the primary collisions and string fragmentations in the microscopic UrQMD model. This leads to non-trivial velocity and energy density distributions for the hydrodynamical initial conditions [24,25]. Subsequently, a full $(3+1)$-dimensional ideal hydrodynamic evolution is performed using the SHASTA algorithm [26,27]. The hydrodynamic evolution is gradually merged into the hadronic cascade: to mimic an iso-eigentime hypersurface, full transverse slices, of thickness $\Delta z = 0.2$ fm, are transformed to particles whenever in all cells of each individual slice the energy density drops below five times the ground state energy density. The employment of such gradual transition allows to obtain a rapidity independent transition temperature without artificial time dilatation effects [28] and has been explored in detail in various recent works [28–31] devoted to SPS conditions. When merging, the hydrodynamic fields are transformed to particle degrees of freedom via the Cooper–Frye equation in the computational frame. The created particles proceed in their evolution in the hadronic cascade where rescatterings and final decays occur until all interactions cease and the system decouples.

An input for the hydrodynamical calculation is the equation of state (EoS). In this work we employ a hadron gas equation of state, describing a non-interacting gas of free hadrons [32]. Included here are all reliably known hadrons with masses up to ≈ 2 GeV, which is equivalent to the active degrees of freedom of the UrQMD model.

The hydrodynamic description of the (pre-transition) hot and dense hadron matter may or may not be valid. Whereas in the low temperature hadron phase large values of the share viscosity to entropy density ratio η/s are consensually expected [33–37], uncertainties are present around the critical temperature. Recent calculations showed that the inclusion of all the known high mass particles and resonances [36,38] in typical hadron resonance gas models leads to lower values of η/s than in the case of a simple gas of pions and nucleons [39]. Adding Hagedorn states [38], or introducing scaled hadron masses and couplings [37], small values of η/s may be reached in the hadron phase. These results are, however, in contrast to the outcome of the Kubo analysis of the UrQMD hadronic transport model, where values of $\eta/s \gtrsim 1$ where found [35]. In addition, accounting for multiparticle processes might further lower the value of η/s for the hadron matter. For these reasons we consider that a hydrodynamical description of the hot and dense hadronic phase is still worth pursuing as a complementary tool to the full hadronic transport description.

In the hadronic cascade phase the dynamics of the ϕ meson proceeds as described in Refs. [21] and [22]: production and decay run through the following channels: $\phi \leftrightarrow \gamma\eta$, $\phi \leftrightarrow \rho\pi$, $\phi \to 3\pi$, $\phi \leftrightarrow K\bar{K}$ (see Tables 3.7 and 3.8 of Ref. [21], string $\to \phi + X$. Elastic and inelastic scattering of the ϕ meson with mesons and baryons are modelled on the basis of the Additive Quark Model (AQM). Values for the total cross sections calculated from the AQM can be found in Tables 4 and 5 of Ref. [22].

2.2. Reconstruction of the ϕ meson in the dimuon channel

The reconstruction of the ϕ meson from the dimuon channel requires the evaluation of the $\phi \to \mu^+\mu^-$ emission. This is calculated perturbatively in the evolution stage that precedes or follows the hydrodynamical phase, and from thermal rates in the latter. In the following, the terms pre-equilibrium/pre-hydro (post-equilibrium/post-hydro), will be used to indicate the stage preceding (following) the mapping UrQMD→hydrodynamical (hydrodynamical→UrQMD) evolution description. Note that in the pre- and post-hydro stages the particles are the explicit degree of freedom and their interactions are explicitly treated within the cascade transport approach.

2.2.1. Reconstruction from pre-equilibrium and post-equilibrium emission

Given the number $N^{\phi}_{\mu^+\mu^-}$ of $\mu^+\mu^-$ pairs emitted in $\phi \to \mu^+\mu^-$ decays, the number $N^{\rm rec}_{\phi}$ of ϕ meson reconstructed in the dimuon channel is

$$N^{\rm rec}_{\phi} = N^{\phi}_{\mu^+\mu^-}/BR^{\phi}_{\mu^+\mu^-}, \tag{1}$$

where $BR^{\phi}_{\mu^+\mu^-}$ is the $\phi \to \mu^+\mu^-$ branching ratio. The latter is given by the ratio between the dimuon and the total width of the ϕ meson, i.e. $BR^{\phi}_{\mu^+\mu^-} = \Gamma^{\phi}_{\mu^+\mu^-}/\Gamma^{\phi}_{\rm tot}$. Thus,

$$N^{\rm rec}_{\phi} = N^{\phi}_{\mu^+\mu^-}\frac{\Gamma^{\phi}_{\rm tot}}{\Gamma^{\phi}_{\mu^+\mu^-}}. \tag{2}$$

In the pre-equilibrium and post-equilibrium phase dimuon emission from the ϕ-meson can be calculated perturbatively as

$$N^{\phi}_{\mu^+\mu^-} = \sum_{n}^{N_{\phi}} \int_{\tau_i(n)}^{\tau_f(n)} \Gamma^{\phi}_{\mu^+\mu^-}\, d\tau \tag{3}$$

where now N_{ϕ} indicates the number of ϕ mesons present, in some stage of the evolution, in the system and $\tau_i(n)$ ($\tau_f(n)$) are the times at which the n-th ϕ meson appeared in (disappeared from) the system and are evaluated in the meson rest-frame. This perturbative method is known as time integration method or "shining method" and has long been applied in the transport description of dilepton emission (see e.g. [40–42]). Combining Eqs. (1)–(3) one has:

$$N_{\phi}^{\mathrm{rec}} = \sum_{n}^{N_{\phi}} \int_{\tau_i(n)}^{\tau_f(n)} \Gamma_{\mathrm{tot}}^{\phi}\, d\tau \tag{4}$$

which expresses the fact that the number of reconstructed mesons is proportional to the typical life-time of the meson in the system.

Some considerations are now in order. During the pre-equilibrium phase, $\tau_i(n)$ coincides with the time at which a ϕ meson is typically produced from a nucleon–nucleon scattering. With exception of some very rare almost instantaneous interaction, $\tau_f(n)$ typically coincides with the time at which the hydrodynamical phase starts. In other words, the probability of dimuon emission in the pre-hydro stage is evaluated up to the moment ϕ mesons are merged into the hydrodynamical phase. From then on, ϕ emission will be treated as thermal.

In the post-equilibrium phase, $\tau_i(n)$ coincides either with the time at which the transition from the hydrodynamical to the transport description is performed (for those ϕ mesons produced via the Cooper–Frye equation) or with the time at which a ϕ meson is produced from hadronic interactions still occurring in the cascade phase, as result of the fact that the whole system is not yet completely decoupled; $\tau_f(n)$ is, in this case, the time at which the ϕ meson decays or eventually rescatters.

2.2.2. Reconstruction from equilibrated thermal emission

Thermal dimuon emission from the ϕ meson can be expected to be significantly smaller than the post-equilibrium emission, due to the fact that the lifetime of the fireball (7–10 fm) is much smaller than the ϕ (vacuum) lifetime of $\sim$ 44 fm. To determine the thermal dimuon production rate from ϕ-meson decays we observe that the mass of the ϕ meson ($m_{\phi} = 1.019$ GeV) is larger than the typical local temperature of the thermalized fireball, thus the particle number distribution function can be reasonably evaluated in Boltzmann approximation. Moreover, the ϕ meson being a very narrow resonance ($\Gamma_{\mathrm{tot}}^{\phi} = 0.00426$ GeV and $\Gamma_{\mathrm{tot}}^{\phi}/m_{\phi} \approx 0.4\%$), for simplicity we neglect its small width and approximate the mass distribution of the meson with a $\delta(m^2 - m_0^2)$ function (pole approximation).

In the Boltzmann and pole approximation the ϕ particle phase space distribution function is given by

$$\frac{dN_{\phi}}{d^3x\, d^3q}\big(q_0; T(\mathbf{x},t)\big) = \frac{3}{(2\pi)^3} e^{-q_0/T(\mathbf{x},t)}, \tag{5}$$

where $T(\mathbf{x},t)$ is the local temperature, $(q_0, \mathbf{q})$ the meson 4-momentum in the thermal frame and the dependence of the temperature from the (discretized) space–time point of the $(3+1)$ grid has been explicitly indicated. The number of dimuons produced per unit phase space volume and unit time from $\phi \to \mu^+\mu^-$ decays is

$$\frac{dN_{\mu^+\mu^-}}{d^4x\, d^3q}\big(q_0; T(\mathbf{x},t)\big) = \frac{dN_{\phi}}{d^3x\, d^3q} \frac{\Gamma_{\mu^+\mu^-}^{\phi}}{\gamma_{\phi}(q_0)}. \tag{6}$$

Here $\Gamma_{\mu^+\mu^-}^{\phi}$ is the dimuon width as defined in the meson rest-frame and $\gamma_{\phi} = q_0/m_{\phi}$ is the Lorentz factor transforming from the meson to the thermal rest frame. The number of dimuons emitted per unit space–time volume can be obtained by integrating Eq. (6) over momentum. The integration can be performed analytically and one finds:

$$\frac{dN_{\mu^+\mu^-}}{d^4x}\big(T(\mathbf{x},t)\big) = \frac{3}{2\pi^2}\, m_{\phi}^2\, T(\mathbf{x},t) K_1\left(\frac{m_{\phi}}{T(\mathbf{x},t)}\right) \Gamma_{\mu^+\mu^-}^{\phi}, \tag{7}$$

where K_1 is the modified Bessel function of first order. The contribution of a single cell to the dimuon emission in the time step Δt is therefore:

$$(N_{\mu^+\mu^-})_{\mathrm{cell}} = \frac{dN_{\mu^+\mu^-}}{d^4x}(T_{\mathrm{cell}})\; V_{\mathrm{cell}} \Delta t. \tag{8}$$

The cell contribution to the dimuon emission is calculated according to the above expression. To compare with experimental data, dimuon momenta in the c.m. frame are then generated with a Monte Carlo procedure according to the distribution function

$$\frac{dN_{\mu^+\mu^-}}{d^3x\, d^3p} \sim \frac{m_{\phi}}{p_0} f_B\left(\frac{p_{\nu} u^{\nu}}{T_{\mathrm{cell}}}\right) \tag{9}$$

with u^{ν} the fluid cell 4-velocity and f_B the boson distribution function.

The total dimuon yield from thermal ϕ mesons is obtained summing the above expression over all fluid cells and all time steps of the $(3+1)$ grid that are spanned by the system during the hydrodynamical evolution until the transition criterium is reached. Let us express this summation symbolically as:

$$N_{\mu^+\mu^-}^{\phi} = \int_{V \subset \mathbb{R}^4} d^4x \left\{ \frac{3}{2\pi^2}\, m_{\phi}^2 T(\mathbf{x},t) K_1\left(\frac{m_{\phi}}{T(\mathbf{x},t)}\right) \Gamma_{\mu^+\mu^-}^{\phi} \right\}. \tag{10}$$

The corresponding number of ϕ mesons reconstructed in the dimuon channel is then:

$$N_{\phi}^{\mathrm{rec}} = \int_{V \subset \mathbb{R}^4} d^4x \left\{ \frac{3}{2\pi^2} m_{\phi}^2 T(\mathbf{x},t) K_1\left(\frac{m_{\phi}}{T(\mathbf{x},t)}\right) \Gamma_{\mathrm{tot}}^{\phi} \right\}. \tag{11}$$

Before proceeding, we would like to make two considerations. The first one concerns an implication of the EoS used for the hydrodynamical evolution. As previously stated, a hadronic EoS has been used in the present work. This implies that dimuon emission from the ϕ meson is here evaluated during the whole hydrodynamical phase. In general, however, if a phase transition from quark–gluon to hadronic matter occurs, the hadronic thermal rate would be only a fraction of the total thermal rate. In this sense, the results presented in the next section on thermal dimuon emission from the ϕ meson should be regarded as an upper limit of the possible amount of dimuons indeed produced by ϕ mesons during the high temperature/high density stage of the heavy-ion collision.

The second consideration regards the validity of the pole approximation used. This approximation is justified as long as the ϕ meson maintains its property of a narrow resonance. In medium, the ϕ meson is expected to broaden, as suggested by hadronic many body calculations. If the amount of broadening is significant or/and the spectral function of the meson develops a complex "structured" shape in the medium, the pole approximation may loose validity. On a quantitative base, there is no general consensus on the specific amount of broadening of the ϕ meson spectral function to be expected in a high temperature/high density environment. Early evaluations of medium effects based on hadronic rescattering at finite temperature have indicated quite moderate changes of both the ϕ meson mass and width [43–46]. In a subsequent calculation, collision rates in a meson gas have been estimated to amount to a broadening by $\sim$ 20 MeV at $T = 150$ MeV [47]. As a consequence, the ϕ mean free path in the hot meson gas was found significantly small. Including all the possible collisions of the ϕ with the hadronic medium analyzed in [47] as well as further in-medium modification of masses of kaons and ϕ mesons in a hadron transport model, Pal et al. [48] showed that ϕ mesons are largely produced and absorbed during the initial high density stage of the collision; moreover, the predominant scattering and absorption of the kaons originating from the ϕ meson decay in the dense hadronic medium together with the in-medium modification of the masses enhance the ϕ meson yield via the dimuon channel compared to that via the dikaon

channel. The dressing of the kaon cloud is presumably the main effect for ϕ modifications in nuclear matter, increasing its width by $\sim$ 25 MeV at normal nuclear density [49]. In hot and baryon poor hadronic matter the in-medium properties of the ϕ have been schematically explored in Ref. [50]: the meson was found to retain its resonance structure and an in-medium width of $\sim$ 32 MeV at $(T, \mu_N) = (180, 27)$ MeV was estimated. In a recent work [51], the spectral density of the ϕ meson in a hot bath of nucleons and pions has been microscopically calculated from the forward scattering amplitude in a two component approach. The authors found a considerable broadening of the meson width, e.g., $\Gamma^{\phi}_{\rm med} \sim 100$ MeV at saturation density and temperature $T = 150$ MeV.

In fact, there is no visible evidence for a strong in-medium scenario for the ϕ meson from the NA60 data. For all the analyzed centrality bins, the measured invariant mass distribution can be described in terms of a vacuum-like spectral function and the extracted values for the mass and the width are compatible with the PDG values and independent of centrality. Of course, one should remind that the extraction of the in-medium modified component of the total dimuon emission from the experimental data is a non-trivial task, since this component would lie under the large unmodified peak produced from the decays occurring at the freeze-out. Certainly, the study of in-medium modifications of the ϕ meson properties is in itself an interesting research topic. However, in the present work we will not address this issue and assume that also in-medium the resonance maintains its narrow width, so that the pole approximation is still valid. For the meson pole mass m_ϕ, moreover, the vacuum value will be used. In any case, as we will show below, from our analysis it emerges that the amount of ϕ's from thermal emission is by far smaller than the abundance from the cascade part, so that an eventual in-medium modification of the thermal rate will most likely not alter the results on the total transverse mass spectra discussed in the next section.

3. Results

In this section we investigate the relative abundances of $\phi \to \mu^+\mu^-$ production in the various stages of the system evolution and present results for ϕ meson invariant transverse mass spectra as a function of the collision centrality. Calculations for $\phi \to \mu^+\mu^-$ production in In–In collisions at $E_{\rm lab} = 158A$ GeV have been performed for 5 centrality classes. In agreement with the treatment of the experimental data, each class was identified by the range of charged particle multiplicity $dN_{ch}/d\eta$ in the pseudorapidity interval $3 \leqslant \eta \leqslant 4$. The relation between a specific range of $dN_{ch}/d\eta$ and the corresponding centrality bin was specified by the NA60 Collaboration and can be found in Table 1 of Ref. [16]. The correspondence between the 5 ranges of $dN_{ch}/d\eta$ and 5 ranges of impact parameters was obtained by the analysis of the charged particles obtained within the UrQMD hybrid model as a function of the impact parameter selected in the Monte Carlo simulation.

3.1. Relative abundances in the various evolution stages and m_T spectra

First, let us investigate the relation between the amount of ϕ mesons reconstructed from $\phi \to \mu^+\mu^-$ and the stage of the evolution probed by the dimuon emission. We start by discussing separately and in detail results for the most central bin. Later, an analogous analysis is presented as function of centrality.

The contribution to the ϕ transverse mass spectra of those ϕ mesons emitting during the hydrodynamical and the cascade stage are separately shown in Fig. 1. The emission from the hydrodynamic stage is found almost one order of magnitude smaller than the emission from the cascade. As already mentioned, this is due to the relative smallness of the duration of the hydrodynamical

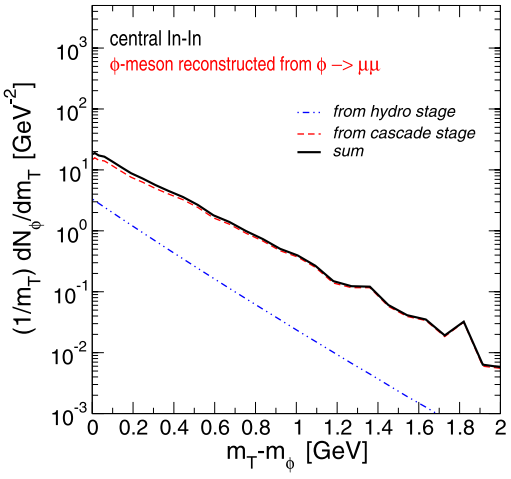

Fig. 1. Transverse mass distributions of the ϕ meson in central indium–indium collisions. The ϕ is reconstructed in the dimuon channel (see text). Double-dotted-dashed line: contribution to the $\phi \to \mu^+\mu^-$ production of the hydrodynamical stage. Dashed line: contribution of the cascade stage. Full line: total $\phi \to \mu^+\mu^-$ production.

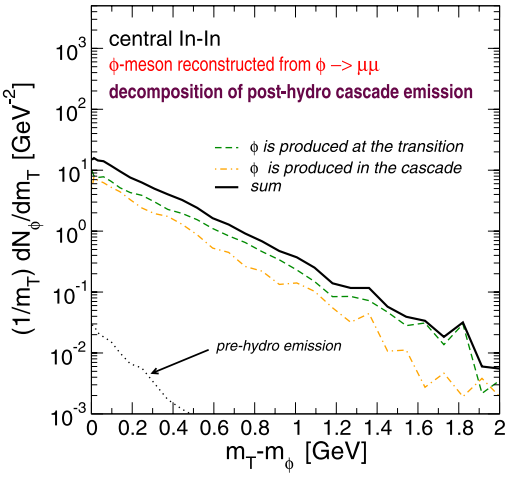

Fig. 2. Decomposition of the post-equilibrium $\phi \to \mu^+\mu^-$ production in: (i) emission from ϕ mesons which are merged into the cascade at the transition point via the Cooper–Frye equation and emit in the cascade stage of the evolution (dashed line); (ii) emission from ϕ mesons which are produced and emit in the cascade stage (dotted-dashed line). The pre-equilibrium emission is denoted by the dotted line. The full line represents the total cascade emission. Due to the smallness of the pre-equilibrium emission the latter practically coincides with the total post-equilibrium emission.

phase when compared to the cascade phase. Thus, the dominant contribution comes from the cascade stage. This stage contains pre- and post-equilibrium emission. However, as shown in Fig. 2, the pre-equilibrium emission is negligible (two orders of magnitude smaller than the post-equilibrium emission) and will not be discussed further. The post-equilibrium emission can be divided in two categories: (i) the emission from ϕ particles produced via Cooper–Frye at the transition point and (ii) the emission from ϕ particles produced *during* the cascade (Fig. 2). In the first case, the particles have a momentum distribution that reflects the thermal properties of the transition point, although their dimuon decay occurs later in a non-thermal environment. In this sense, this copious emission, though not specifically thermal (i.e. not described by thermal rate equations) still carries information about the preceding thermal phase. It represents the most direct "remain" of the thermally equilibrated phase previously experienced by the sys-

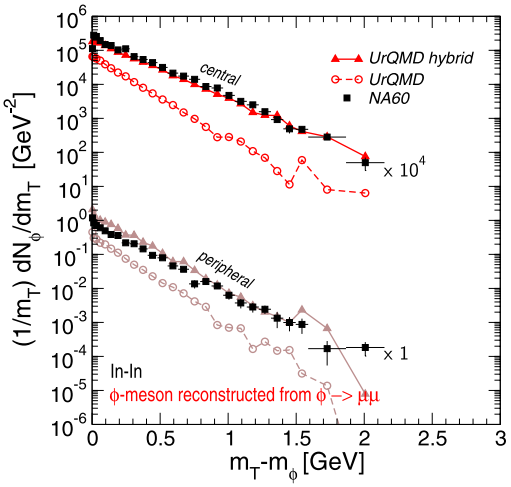

Fig. 3. Transverse mass distributions of the ϕ meson in central (top) and peripheral (bottom) indium–indium collisions. The hybrid model calculation (full line) is compared to the pure UrQMD transport calculation (dashed line) and to experimental data [16]. Bin-widths which coincide with the ones of the experimental data have been here used.

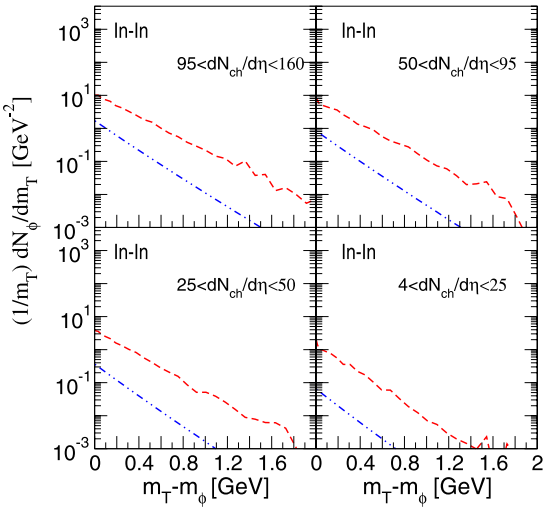

Fig. 4. Same as in Fig. 1, but for different centrality classes. Double-dotted-dashed line: contribution to the $\phi \to \mu^+\mu^-$ production of the hydrodynamical stage. Dashed line: contribution of the cascade stage.

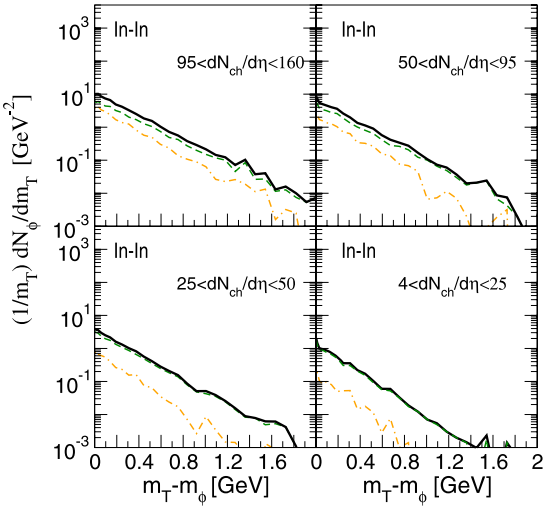

Fig. 5. Same as in Fig. 2, but for different centrality classes. Dashed line: emission from ϕ mesons which are merged into the cascade at the transition point via the Cooper–Frye equation and emit in the cascade stage of the evolution; Dotted-dashed line: emission from ϕ mesons which are produced and emit in the cascade stage.

tem. The second contribution, on the contrary, can be labeled as a "purely cascade" one. This is the contribution of ϕ particles produced in the non-equilibrium environment on the way to final decoupling. This second contribution is characterized by steeper transverse mass spectra. The shape of the total spectra is found to be composed by the interplay of both emissions.

It is instructive to compare the hybrid model calculations to the pure cascade calculations, in which no assumption of an intermediate equilibrium phase is made. The comparison is presented in Fig. 3 (top) together with the experimental data. As one can see, the absence of an intermediate thermal phase results in a steepening of the transverse mass spectra not supported by the data. Moreover, the pure cascade calculation strongly underestimates the ϕ meson yield, a feature already emerged in recent independent investigations [13] performed in relation to measurements obtained by the NA49 experiment. There, it was found that a statistical hadron gas model with undersaturation of strangeness [52] could account for the measured yields [13]. In this respect, however, it should be mentioned that the UrQMD model underestimates ϕ meson yield at high energies already in $p+p$ collisions [22]. The results clearly show that, even in the most central collisions, this initial state "information" is not fully lost through subsequent collisions in the UrQMD description. On the other hand, in the previously mentioned work of Pal et al., in which appreciably large collisional rates of the ϕ were added, it was found that the ϕ meson abundancies is totally determined by the purely hadronic rescattering already at $t = 10$ fm and independent from the inclusion or not of initial ϕ mesons from string decays.

From this first analysis, we can conclude that, despite the smallness of the specifically thermal $\phi \to \mu^+\mu^-$ emission, the presence of the thermal phase is essential in order to obtain an appropriate yield and slope of the m_T distributions from the cascade emission. In this sense, we speak about the presence of "thermal relics".

An analogous analysis has been performed for the further 4 centrality bins and results are presented in Fig. 4 and 5. For all centrality classes the thermal rate from the hydrodynamic evolution is found to be much smaller than the cascade emission. With decreasing centrality, the pure cascade emission (dash-dotted line) becomes less and less important and the spectra is more and more determined by the emission from those mesons emerging from the thermal stage into the cascade at the transition point.

The ϕ meson transverse mass spectra calculated within the hybrid model for the 5 centrality classes considered are compared to NA60 data in Fig. 6. The hybrid model can account pretty well for both slope and yield in the first 4 centrality classes. Small deviations are observed for the utmost peripheral bin where, most likely, this kind of hybrid models are already at the limit of applicability. They rely on the assumption that an equilibrium phase is indeed reached, which for very peripheral reactions is at least questionable [53].

Pure transport calculations fail however too in describing this very peripheral reaction (see Fig. 3, bottom), though the comparison with experimental data suggests that deviations of the resulting slope from the measured one are much smaller than the in the case of central collisions.

In Fig. 7, finally, we show the total number of ϕ mesons reconstructed in the dimuon channel as well as their average transverse mass for the five centrality classes. The number of participants corresponding to each class have been taken from Ref. [16]. The

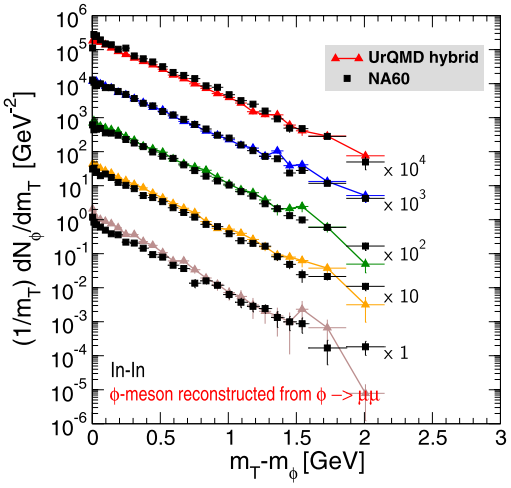

Fig. 6. Transverse mass distributions of the ϕ meson in indium–indium collisions as a function of centrality; from top to bottom: central to peripheral spectra. The hybrid model calculations are compared with NA60 data [16]. Bin-widths which coincide with the ones of the experimental data have been here used.

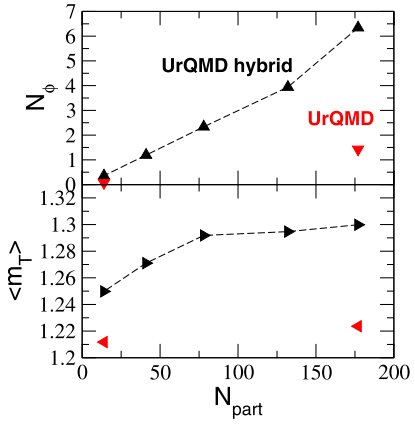

Fig. 7. ϕ meson multiplicity (upper panel) and average transverse mass (lower panel) as a function of centrality. Results of the hybrid (symbols with lines) and the pure cascade (only symbols) approach are shown.

increase of yield with centrality is comparable in the two models: the ratio $(N_\phi)_{central}/(N_\phi)_{peripheral}$ is $1.43/0.07 \sim 20$ in the UrQMD calculation and $6.34/0.36 \sim 18$ in the hybrid model one. The mean transverse mass is always larger in the hybrid calculation due to the more violent expansion dynamics. This corresponds to flatter m_T spectra which are in line with the experimental data as it has been discussed above. Moreover, the increase of mean transverse mass with centrality is more pronounced in the hybrid calculation.

4. Summary and conclusions

In this work we employed an integrated Boltzmann+hydrodynamics hybrid approach based on the Ultrarelativistic Quantum Molecular Dynamics transport model with an intermediate hydrodynamic stage to analyze ϕ-meson production in In+In collisions at $E_{\rm lab} = 158A$ GeV from its reconstruction in the $\phi \to \mu^+\mu^-$ channel. We find that the hybrid model fairly describes ϕ yields and transversal mass spectra at various collision centralities. In particular, the analysis points out that the underlying assumption of the existence of an intermediate equilibrated phase seems to play an essential role in order to catch the main aspects of the physics emerging from the ϕ dimuon emission at top SPS energies.

Acknowledgements

The authors acknowledge G. Torrieri and P. Huovinen for fruitful discussions, the NA60 Collaboration, M. Floris in particular, for providing the experimental data and D.H. Rischke for providing the hydrodynamics code. This work was supported by BMBF, GSI, DFG and the Hessen Initiative for Excellence (LOEWE) through the Helmholtz International Center for FAIR (HIC for FAIR). We thank the Center for Scientific Computing for the computational resources.

References

[1] J. Rafelski, B. Muller, Phys. Rev. Lett. 48 (1982) 1066.
[2] P. Koch, B. Muller, J. Rafelski, Phys. Rept. 142 (1986) 167.
[3] A. Shor, Phys. Rev. Lett. 54 (1985) 1122.
[4] S. Okubo, Phys. Lett. 5 (1963) 165.
[5] G. Zweig, CERN report 8419/Th (1964) 412.
[6] J. Iizuka, Prog. Theor. Phys. Suppl. 37 (1966) 21.
[7] Y. Cheng, F. Liu, Z. Liu, K. Schweda, N. Xu, Phys. Rev. C 68 (2003) 034910.
[8] T. Hirano, U.W. Heinz, D. Kharzeev, R. Lacey, Y. Nara, Phys. Rev. C 77 (2008) 044909, arXiv:0710.5795.
[9] H. van Hecke, H. Sorge, N. Xu, Phys. Rev. Lett. 81 (1998) 5764, nucl-th/9804035.
[10] S.V. Afanasev, et al., NA49 Collaboration, Phys. Lett. B 491 (2000) 59.
[11] V. Friese, NA49 Collaboration, Nucl. Phys. A 698 (2002) 487.
[12] C. Alt, et al., NA49 Collaboration, Phys. Rev. Lett. 94 (2005) 052301, nucl-ex/0406031.
[13] C. Alt, et al., NA49 Collaboration, Phys. Rev. C 78 (2008) 044907, arXiv:0806.1937.
[14] D. Adamova, et al., CERES Collaboration, Phys. Rev. Lett. 96 (2006) 152301, nucl-ex/0512007.
[15] B. Alessandro, et al., NA50 Collaboration, Phys. Lett. B 555 (2003) 147.
[16] R. Arnaldi, et al., NA60 Collaboration, Eur. Phys. J. C 64 (2009) 1, arXiv:0906.1102.
[17] S.C. Johnson, B.V. Jacak, A. Drees, Eur. Phys. J. C 18 (2001) 645, nucl-th/9909075.
[18] E. Santini, G. Burau, A. Faessler, C. Fuchs, Eur. Phys. J. A 28 (2006) 187, nucl-th/0605041.
[19] P. Filip, E.E. Kolomeitsev, Phys. Rev. C 64 (2001) 054905, hep-ph/0107288.
[20] H. Petersen, J. Steinheimer, G. Burau, M. Bleicher, H. Stocker, Phys. Rev. C 78 (2008) 044901, arXiv:0806.1695.
[21] S.A. Bass, et al., Prog. Part. Nucl. Phys. 41 (1998) 255, nucl-th/9803035.
[22] M. Bleicher, et al., J. Phys. G 25 (1999) 1859, hep-ph/9909407.
[23] H. Petersen, M. Bleicher, S.A. Bass, H. Stocker, 2008; arXiv:0805.0567.
[24] J. Steinheimer, et al., Phys. Rev. C 77 (2008) 034901, arXiv:0710.0332.
[25] H. Petersen, M. Bleicher, Phys. Rev. C 79 (2009) 054904, arXiv:0901.3821.
[26] D.H. Rischke, S. Bernard, J.A. Maruhn, Nucl. Phys. A 595 (1995) 346, nucl-th/9504018.
[27] D.H. Rischke, Y. Pursun, J.A. Maruhn, Nucl. Phys. A 595 (1995) 383, nucl-th/9504021.
[28] H. Petersen, J. Steinheimer, G. Burau, M. Bleicher, Nucl. Phys. A 830 (2009) 283c, arXiv:0907.2169.
[29] Q.-f. Li, J. Steinheimer, H. Petersen, M. Bleicher, H. Stocker, Phys. Lett. B 674 (2009) 111, arXiv:0812.0375.
[30] H. Petersen, J. Steinheimer, M. Bleicher, H. Stocker, J. Phys. G 36 (2009) 055104, arXiv:0902.4866.
[31] H. Petersen, J. Steinheimer, G. Burau, M. Bleicher, Eur. Phys. J. C 62 (2009) 31.
[32] D. Zschiesche, S. Schramm, J. Schaffner-Bielich, H. Stoecker, W. Greiner, Phys. Lett. B 547 (2002) 7, nucl-th/0209022.
[33] M. Prakash, M. Prakash, R. Venugopalan, G. Welke, Phys. Rept. 227 (1993) 321.
[34] T. Hirano, M. Gyulassy, Nucl. Phys. A 769 (2006) 71, nucl-th/0506049.
[35] N. Demir, S.A. Bass, Phys. Rev. Lett. 102 (2009) 172302, arXiv:0812.2422.
[36] M.I. Gorenstein, M. Hauer, O.N. Moroz, Phys. Rev. C 77 (2008) 024911, arXiv:0708.0137.
[37] A.S. Khvorostukhin, V.D. Toneev, D.N. Voskresensky, 2009; arXiv:0912.2191.
[38] J. Noronha-Hostler, J. Noronha, C. Greiner, Phys. Rev. Lett. 103 (2009) 172302, arXiv:0811.1571.
[39] K. Itakura, O. Morimatsu, H. Otomo, Phys. Rev. D 77 (2008) 014014, arXiv:0711.1034.
[40] G.-Q. Li, C.M. Ko, Nucl. Phys. A 582 (1995) 731, nucl-th/9407016.
[41] S. Vogel, et al., Phys. Rev. C 78 (2008) 044909, arXiv:0710.4463.
[42] K. Schmidt, et al., Phys. Rev. C 79 (2009) 064908, arXiv:0811.4073.

[43] C.M. Ko, D. Seibert, Phys. Rev. C 49 (1994) 2198, nucl-th/9312010.
[44] K.L. Haglin, C. Gale, Nucl. Phys. B 421 (1994) 613, nucl-th/9401003.
[45] K. Haglin, Nucl. Phys. A 584 (1995) 719, nucl-th/9410028.
[46] W. Smith, K.L. Haglin, Phys. Rev. C 57 (1998) 1449, nucl-th/9710026.
[47] L. Alvarez-Ruso, V. Koch, Phys. Rev. C 65 (2002) 054901, nucl-th/0201011.
[48] S. Pal, C.M. Ko, Z.-w. Lin, Nucl. Phys. A 707 (2002) 525, nucl-th/0202086.
[49] D. Cabrera, M.J. Vicente Vacas, Phys. Rev. C 67 (2003) 045203, nucl-th/0205075.
[50] R. Rapp, Phys. Rev. C 63 (2001) 054907, hep-ph/0010101.
[51] G. Vujanovic, J. Ruppert, C. Gale, Phys. Rev. C 80 (2009) 044907, arXiv:0907.5385.
[52] F. Becattini, J. Manninen, M. Gazdzicki, Phys. Rev. C 73 (2006) 044905, hep-ph/0511092.
[53] H. Petersen, M. Mitrovski, T. Schuster, M. Bleicher, Phys. Rev. C 80 (2009) 054910, arXiv:0903.0396.